BALLOON-BORNE DIRECT SEARCH FOR IONIZING MASSIVE PARTICLES AS A COMPONENT OF THE GALACTIC HALO DARK MATTER

P.C. McGuire[1,7], T. Bowen[1], D.L. Barker[1], P.G. Halverson[1,6], K.R. Kendall[1], T.S. Metcalfe[1], R.S. Norton[1], A.E. Pifer[1], L.M.Barbier[2], E.R.Christian[2], K.E.Krombel[2], J.W. Mitchell[2], J.F. Ormes[2], R.E. Streitmatter[2], A.J. Davis[3], A.W. Labrador[3], R.A. Mewaldt[3], S.M. Schindler[3], R.L. Golden[4], S.J. Stochaj[4], W.R. Webber[4,5]

(The Arizona-IMAX Collaboration)

[1]Department of Physics, University of Arizona, Tucson AZ 85721

[2]Laboratory for High Energy Astrophysics, NASA Goddard Space Flight Center (GSFC), Code 661, Greenbelt, MD 20771

[3]Space Radiation Laboratory, California Institute of Technology, Pasadena, CA 91125

[4]Particle Astrophysics Laboratory, New Mexico State University, Las Cruces, NM 88003

[5]Astronomy Department, New Mexico State University, Las Cruces, NM 88003

[6]Physics Department, University of California at Irvine, Irvine, CA 92717

[7]EMAIL: Internet – mcguire@soliton.physics.arizona.edu or DECnet – UAZHEP::MCGUIRE

A dark matter (DM) search experiment was flown on the IMAX balloon payload, which tested the hypothesis that a minor component of the dark matter in the Galactic halo is composed of ionizing massive particles (IMPs) (with $dE/dx > 1$ MeV/g/cm^2 or $\sigma > 2 \times 10^{-20}$ cm^2; $m_x \in [10^4, 10^{12}]$ GeV/c^2) that cannot penetrate the atmosphere due to their low-velocities ($\beta \in [0.0003, 0.0025]$). The DM search experiment consisted of a delayed coincidence between four $\sim$ 2400 cm^2 plastic scintillation detectors arranged in a vertical 2.5 m stack, with a total acceptance of 100 cm^2 sr. In order to search for ultra-slow particles which do not slow down in the IMAX telescope, the experiment contained TDCs which measured the time-delays $T_{i,i+1} \in [0.3, 14.0]$ μs between hits in successive counters to $\sim 2\%$ precision. Using the first 5 hours of data at float altitude (5 g/cm^2 residual atmosphere), we observed 5 candidate non-slowing and 16 candidate slowing dark matter particle events, consistent with the background expected from accidental coincidences of 4.0 non-slowing and 18.3 slowing events. This implies that the DM flux is less than 6.5×10^{-6} cm^{-2}s^{-1}sr^{-1} (95% C.L.) for non-slowing IMPs ($\sigma/m_x < 2.31 \times 10^{-26}$ cm^2/GeV); and the DM flux is less than 7.9×10^{-6} cm^{-2}s^{-1}sr^{-1} (95% C.L.) for slowing IMPs ($\sigma/m_x < 2.1 \times 10^{-25}$ cm^2/GeV). This experiment effectively closes much of a previously unconstrained 'window' in the mass/cross-section joint parameter space for massive particles as the dominant halo DM, and implies that for certain regions of this parameter space, massive particles cannot be more than one part in 10^5 by mass of all the DM. These results can also directly constrain 'light' magnetic monopoles, neutral hadrons and neutraCHAMPs in a previously unconstrained mass region $m_x \in [10^6, 10^8]$ GeV.

1 INTRODUCTION

Our solar system rotates around the Galactic center much swifter than theory predicts (with the assumption that our motion around the Galactic center is only due to the gravitational pull from all the other stars and hydrogen gas in our Galaxy). Therefore, many scientists hypothesize a cloud of 'invisible' dark matter that would surround our Galaxy and enhance the Galaxy's gravitational well and the rotational velocity of our Galaxy, in accord with observation. For example, one model[1][2] predicts that if the dark matter halo is spherically symmetric, then the density of dark matter halo in the solar neighborhood is:

$$\rho \in [4 \times 10^{-3}, 10^{-2}]\ M_\odot/\mathrm{pc}^3 \equiv [2.4, 7.4] \times 10^{-25}\ \mathrm{g/cm}^3 \equiv [0.17, 0.42]\ \mathrm{GeV/cm}^3, \quad (1)$$

which is equivalent to a flux of

$$\Phi \in [1.0, 2.5] \times \frac{10^6\ \mathrm{GeV}}{m_x}\ \mathrm{cm}^{-2}\mathrm{s}^{-1}\mathrm{sr}^{-1}, \quad (2)$$

where m_x is the mass of the dark matter object in GeV, and the mean speed of the galactic dark matter objects, $\bar{v} \approx 240$ km/s $= 8.0 \times 10^{-4}c$, has been used[32][3]. The flux of the dark matter objects as a function of velocity (ignoring angular dependencies) will follow a 'cut-off' Maxwellian distribution [32][4]:

$$\begin{aligned} \frac{d\Phi}{du} &= 3.6 f_d \text{ cm}^{-2}\text{s}^{-1}\text{sr}^{-1}\Theta(\tfrac{v_{\max}}{\tilde{v}} - u)\, u^3 \exp\left(-u^2\right) \\ &\quad \times \left(\tfrac{\rho}{0.3 \text{ GeV/cm}^3}\right)\left(\tfrac{\tilde{v}}{213 \text{ km/s}}\right)\left(\tfrac{10^6 \text{ GeV}}{m_x}\right) \quad , \end{aligned} \tag{3}$$

where we have used a mid-range value for the dark matter density, $\rho = 0.3$ GeVcm^{-3}, f_d is the fraction of the dark matter halo which the object represents, and $u \equiv v/\tilde{v}$. We will assume a velocity dispersion of $\tilde{v} = \bar{v}\sqrt{\pi}/2 = 213$ km/s and a galactic escape cutoff velocity of $v_{\max} = 640$ km/s[32][3]. If $f_d \sim 1$, then for masses $m_x < 10^6$ GeV the galactic halo dark matter flux in equations 2 and 3 becomes larger than the cosmic ray flux, which has the order of magnitude ~ 1 cm^{-2}s^{-1}sr^{-1}. A whole host of different 'elementary' particles have been hypothesized as solutions to the dark matter problem (e.g. a small rest mass for ordinary neutrinos, WIMPs, technibaryons, monopoles, CHAMPs[20], very massive neutrinos, SIMPs[23][24][25], strange quark nuggets[21], axions); and novel particle detectors are required to detect each different dark matter candidate. Another dark matter candidate, MAssive Compact Halo Objects (MACHOs), has also been proposed [33] and possibly observed [34][35].

Weakly Interacting Massive Particles (WIMPs) (which include cosmions, massive neutrinos, LSPs) are considered by many scientists to be a likely dark matter particle candidate. In the early universe, the low WIMP cross-section would make it quite likely that enough WIMPs could survive annihilation from anti-WIMPs, so as to be abundant enough to solve the missing matter problem today [22]. However, Ionizing Massive Particles (IMPS), which presently have a much higher interaction cross-section with ordinary matter, might have a primodial annihilation cross-section that is similar to the WIMP primordial annihilation cross-section. Therefore, IMPs *might* have a relic abundance that is large enough to constitute all the dark matter in the universe and be unnoticed in past experiments[20][20][24][31][25]. Examples of IMPs include: CHAMPs (electrically CHArged Massive Particles), SIMPs (Strongly Interacting Massive Particles), monopoles and "strange" quark nuggets. If IMPs have antiparticles, the range of IMP masses for which IMPs could be the dominant (halo) dark matter (DDM) includes $m_x \in [6 \times 10^2, 3 \times 10^5]h$ GeV, where $h \sim 1$ is the Hubble constant[20].

Since the high interaction cross-section of IMPs with ordinary nuclei should have easily observable consequences, many experiments have been completed[4]-[19] or clever arguments invented [26]-[30] to rule out different hypothetical IMPs as the DDM, within the theoretically most favored ranges of IMP mass, m_x, number density, n_x, and interaction cross-section with ordinary nuclei σ_{xN}. However, Starkman *et al.* have found that for a significant range of the joint mass and interaction cross-section parameter space, generic IMPs have *not* been ruled out as the dominant halo dark matter, as previously thought.

Furthermore, dark matter might not be restricted to a *single* component; the dark matter halo may be a 'cosmic garbage-dump' for many different supermassive relics (neutron stars, brown dwarfs, black holes, WIMPs, IMPs), including all long-lived particles or objects having a large mass compared to their energy-dissipation rate, preventing collapse into the galactic disk. Why not search for the less dominant forms? If IMPs existed as a very minor component of the dark halo matter, they would be much easier to detect and characterize than WIMPs or MACHOs, for example. Even if WIMPs (with very small cross-sections) are eventually detected by the deep underground searches, it will still be very difficult to extract information about the WIMPs' characteristics[5] (e.g., velocity – both magnitude and direction, and mass).

Therefore, considering the motivations listed above, IMP search experiments need a sensitivity to fluxes many orders-of-magnitude below those given by Equation 2. Due to the high interaction cross-section of IMPs, and their non-relativistic nature ($v_{\text{CDM}} \sim 300$ km/s), a time-of-flight search for very slow IMPs is a plausible method to search for such low fluxes for the mass-range $m_x \in [10^4, 10^{10}]$ GeV. A balloon or satellite-borne experiment is necessary to search for IMPs with a cross-section to mass ratio exceeding $\sigma/m_x \sim 10^{-27}$ cm^2/GeV. We have found the time-of-flight technique using at least 4 scintillation detectors allows us to perform IMP searches that not only are sensitive to very low fluxes, but also allow us to detect IMPs with a relatively small energy loss[38].

Despite the fact that the IMAX dark matter search is similar in spirit and technique to the ground-based experiment by Barish *et al.* [12], our work was unprecedented for several reasons. First and foremost, dark matter hunters have rarely searched for dark matter particles at balloon or satellite altitude. Second, usually when a search for dark matter particles at balloon or satellite altitude has been performed, the experimenters have been unable to reject the background with flux ~ 1 cm^{-2}s^{-1}sr^{-1}

from ordinary cosmic rays, which deposit energies of > 2 MeV/g/cm^2. Our search for IMPs with a four-fold delayed coincidence between the four scintillation detectors in the IMAX stack[38] was the first dark matter particle search experiment flown at balloon altitude which could reject the cosmic ray background to a flux level of $\sim 10^{-5}$ cm^{-2}s^{-1}sr^{-1} and have a relatively small energy-loss threshold (dE/dx (THR) ~ 3.5 MeV/g/cm^2).

We initially searched for neutraCHAMPs as dark matter candidates at mountain altitude, but decided in 1990 that neutraCHAMPs would not likely be able to remain neutral in their flight through the atmosphere and therefore would probably be stopped in the atmosphere above our detectors at mountain altitude. Therefore, we decided to move our neutraCHAMP search to balloon altitude. Fortunately, the IMAX collaboration had a balloon flight planned for the summer of 1991 which had the requisite four scintillation detectors; the IMAX collaborators agreed to add our dark matter particle search experiment to their cosmic ray astrophysics program for antiprotons and light nuclei[39]. At 21.36 hours CDT July 16, 1992, the IMAX payload with our Dark Matter Detector Module (D-Module) was launched by the National Scientific Ballooning Facility (NSBF) from Lynn Lake, Manitoba, Canada for a one-day flight.

This article discusses the results of this balloon-borne dark matter search. In section 2, we discuss IMP energy-loss in scintillation detectors; in section 3 we explain out time-of-flight technique; in section 4 we describe the IMAX apparatus, the IMAX flight parameters and the flight data; and in section 5 we summarize the results of our search for IMPs as dark matter.

2 DESIGN OF THE IMP SEARCH EXPERIMENT

2.1 Parameters of Search

The parameters of the IMAX balloon flight opportunity are listed in Table 1 and the counter arrangement is illustrated in Figure 1. In order for an IMP to reach the experiment and traverse the counter telescope, it must pass through 19 g/cm^2. If dE/dx is its average rate of energy loss, then it must have a kinetic energy, E, satisfying the inequality,

$$E = \frac{1}{2} m_x \beta^2 > 19 \frac{dE}{dx} , \tag{4}$$

or

$$\frac{m_x}{\frac{dE}{dx}} > \frac{38}{\beta^2} \sim 4 \times 10^7 \text{ g/cm}^2, \tag{5}$$

assuming $\beta \approx 10^{-3}$.

Since four successive scintillation counters would be traversed in the IMAX arrangement, three independent velocity measurements can be calculated from the time delays t_{12}, t_{23}, and t_{34}. As $\beta \sim 10^{-3}$ corresponds to velocity $v \sim 0.3\text{m}/\mu\text{s}$, the expected time delays are each of the order of microseconds. If $m_x/(dE/dx)$ is much larger than required for Equation 5, then we would expect $v_{12} \approx v_{23} \approx v_{34}$ for IMPs. If the inequality in Equation 5 is barely satisfied, then we find, assuming that the velocity change Δv from one gap to the next is due to ≈ 5 g/cm^2 of additional material, that

$$\frac{\Delta v}{v} < 0.25 \tag{6}$$

In order to record and analyze such slowing-down events, as well as $\Delta v \approx 0$ events, the IMP search experiment was designed to record all three time delays (see Figure 2), as well as all four scintillation pulse amplitudes.

2.2 Trigger threshold – scintillator saturation

The minimum value of $(dE/dx)_{\beta \sim 0.001}$ to trigger each counter corresponded to a discriminator setting at approximately 35% of the pulse height for minimum ionizing particles – about 0.6 MeV/cm. However, a saturation correction must be made for the relative light of a slow particle passing plastic scintillator. Ficenec *et al.*[44] measured the light yield L in eV of proton recoils with β from 2.5×10^{-4} to 5×10^{-3} in NE-110, extending the measurements of Ahlen and collaborators [45][46] to lower velocities. By direct numerical differentiation of the data reported in these studies, we calculated the scintillation efficiency $(dL/dE)_\beta$ for a proton at velocity β, which we compared with $(dL/dE)_{\beta=1} = 0.03$ for minimum ionizing

particles. We found that for β from 6×10^{-4} to 1.5×10^{-3}, the efficiency, ϵ_Δ, of measuring $\Delta L/\Delta E$ (relative to minimum ionizing particles) is at a local maximum, so it is roughly constant at

$$\epsilon_\Delta(\beta \sim 10^{-3}) = \frac{\left(\frac{dL}{dE}\right)_{\beta \sim 10^{-3}}}{\left(\frac{dL}{dE}\right)_{\beta=1}} = 0.20 \pm 0.05 \tag{7}$$

At higher proton energies, it has been found that a variety of scintillation plastics and liquids have nearly the same saturation curves [48]. The manufacturer has assured us that the Bicron BC-420, 400, 408, and 420 employed in detectors T1, S1, S2, T2, respectively are very nearly the same as NE-110, differing mainly in the wavelength of peak output. The result expressed above in Equation 7 is applicable to protons only while $\beta \sim 10^{-3}$; it should also be valid for any more massive charge $Z = +1$ particle when $\beta \sim 10^{-3}$ (denoted positive CHAMPs by De Rujula *et al.*[20]). Near $\beta \sim 10^{-3}$, the electronic energy loss, which produces most of the scintillation light, varies linearly with β for protons and $Z = +1$ IMPs, and $(dE/dx)_{\beta=0.001,\text{electronic}} = 150$ MeV/cm in scintillator plastic[46]. Multiplying by the saturation correction of Equation 7,

$$\left(\frac{dE}{dx}\right)^{\beta=1 \text{ equiv. of}}_{\beta=10^{-3}} = 30 \text{ MeV equiv./cm.} \tag{8}$$

In other words, since $(dE/dx)^{\beta=1} \approx 1.7$ MeV/cm for minimum ionizing particles in plastic scintillator, a $Z = +1$ IMP would give a signal ~ 15 times minimum ionization at $\beta = 10^{-3}$; therefore, roughly 5 and 50 times minumum ionization at $\beta = 0.33 \times 10^{-3}$ and 3.3×10^{-3}, respectively, the lower and upper limits of velocities accepted by the IMAX search (see Figure 3). Such large pulses would register as overflows in the pulse height ADCs. Using Equation 5 and $(dE/dx)_{\beta=0.001} = 200$ MeV/cm for the total loss rate at $\beta = 10^{-3}$ [46], the mass m_x of $Z = +1$ IMPs would have to be greater than 8 PeV to reach and traverse the counter telescope.

2.3 Threshold for neutral IMPs

The light yield data of Ficenec *et al.*[44] in the β_p range $(0.7 \text{ to } 1.4) \times 10^{-3}$ is well fit by $L_p = 6.4 \times 10^{-3} E_p$, where E_p is the total kinetic energy of the proton recoiling from a neutron scattering; when compared with $L = 0.03 \Delta E$ for minimum ionizing particles, the relative efficiency, $\epsilon_{p,\text{total}}$, of measuring the *total* proton recoil energy is

$$\epsilon_{p,\text{total}}(\beta_p \sim 10^{-3}) = (6.4 \times 10^{-3})/(3 \times 10^{-2}) = 0.21 \text{ for } 0.7 \times 10^{-3} \leq \beta_p \leq 1.4 \times 10^{-3}. \tag{9}$$

This result for ϵ_{total} is slightly higher than for ϵ_Δ in Equation 7 because dE/dx *decreases* as the proton slows down, *increasing* the scintillation efficiency. For the β_p range $(1.4 - -5) \times 10^{-3}$, the data [44][47] are fit by $L_p = (2.3 \times 10^{-2}) E_p^{0.815}$, so $\epsilon_{p,\text{total}}$ is given by

$$\epsilon_{p,\text{total}}(\beta_p) \approx \frac{(1.91 \times 10^{-2})}{\beta_p^{0.37}} \quad \text{for } 1.4 \times 10^{-3} \leq \beta_p \leq 5 \times 10^{-3}. \tag{10}$$

For neutral IMP short-range ($R \ll 210$ fm) interactions at $\beta \sim 10^{-3}$ with protons, the s-wave would be dominant; hence, the scattering would be isotropic in the center-of-mass system and the proton recoil energies would be uniformly distributed between 0 and $2 m_p \beta^2$. With $m_p \beta^2$ mean energy, the proton recoil β_R would have a mean $\langle \beta_p^2 \rangle = 2\beta^2$, so for IMP $\beta \sim 10^{-3}$, $\epsilon_{\text{Total}}(\text{p recoils}) \approx 0.2$.

The scintillator plastic contains roughly equal numbers of hydrogen and carbon atoms; assuming that the IMP–p and IMP–^{12}C interaction matrix elements are comparable, most of the dE/dx would be due to IMP–^{12}C collisions because (a) the density of final states is proportional to reduced mass squared, μ^2, and (b) the energy carried away by the recoil is proportional to μ. For short-range ($R \ll 18$ fm) neutral-IMP interactions with ^{12}C, the scattering is again s-wave and isotropic, and the β_R distribution is the same as for the protons, assuming $m_{\text{IMP}} \gg m_{^{12}\text{C}}$.

2.4 Accidental Coincidences

In order to search for IMPs over a wide range of velocities, 0.1 to 1.0 m/μs $\left[\beta = (0.33 \text{ to } 3.3) \times 10^{-3}\right]$, triggering is accomplished in a specially designed detector module with a series of delayed coincidence

gates, as illustrated in Figure 2. The first gate was generated by each pulse from counter T1; if a pulse from counter S1 arrived within the first gate, a second gate was generated; and if a pulse from counter S2 arrived within the second gate, the event was recorded at the end of the third gate. If a pulse from counter T2 arrived during the third gate, its time delay, t_{34}, and pulse amplitude were recorded along with t_{12}, t_{23}, and the pulse amplitudes of the other counters. All time intervals and pulse heights were stored as charged-capacitor voltages by current-integrating op-amps and sample-and-hold circuits for time intervals and pulse amplitudes, respectively, for readout by an ORTEC 811 ADC CAMAC module. The fourth counter was not required for event recording in order to obtain a sufficiently high event recording rate (~ 4/sec at float altitude) to monitor performance.

The wide coincidence timing gates (μs instead of ns) ensured a steady stream of accidental coincidences uniformly distributed in each time gate, the principal background for the IMP search. The time-ordered accidental rate $A(n)$ for n counters is proportional to each counter's singles rate, R_i, and to the gatewidths, $\tau_{j-1,j}$, for each of the delayed coincidences:

$$A(n) = \prod_{i=1}^{n} R_i \prod_{j=2}^{n} \tau_{j-1,j} \text{ for } n \geq 2 \ , \tag{11}$$

where the customary factor of n does not appear due to the time-ordering requirment. At float altitude, $R_i \approx 3500$ Hz for each counter, and with the gate widths shown in Figure 2, $A(3) \approx 4$ Hz; about 44×10^3 events were recorded (reduced somewhat by deadtime) during the five hours of excellent IMP search data at float altitude. The time interval distributions are shown in Figure 4. The time-interval distributions are uniform, as expected, except for the peaks in T_{12} and T_{23} which are due to anomalous events, of unknown origin, which are eliminated from the data set when the slowness limits, $s_{\min} = 1.5\mu$s/m, $s_{\max} = 10\mu$s/m, corresponding to the limits of the T_{34} distribution, are applied to T_{12} and T_{23}.

Since $R_4\tau_{34} \approx 0.014$ and $A(4) \approx 0.055$ Hz, 653 four-fold accidental coincidences were observed during the five hour observation period. However, if the three independent time measurements must be consistent in the data analysis with the time delays of an IMP traversal within, say, $\pm 1\sigma$, where $\sigma = 2\%$, then two of the timing gates are effectively narrowed; one of the gates is not narrowed since the IMP is allowed to have any velocity consistent with the gate widths. Then $A(4) \sim 3(0.055)(0.04)^2 = 2.6 \times 10^{-4}$ Hz (the factor of 3 accounts for allowing IMP deviations in any order) corresponding to $N_{\rm IMP} \sim 5$ accidental events which mimic IMP traversals in the 5 hours of analysed data. Thus the IMAX time-of-flight IMP search has a maximum detectable flux, $\Phi_{\rm IMP,\ min.\ det.}$, at the 4σ level using $N_{\rm IMP} + N_{\rm ACCID} \geq 14$ as well as the geometry factor Ω and time t from Table 1, given by:

$$\Phi_{\rm IMP,\ min.\ det.} \sim \frac{N_{\rm IMP}}{\Omega t} = 5 \times 10^{-6}\ {\rm cm}^{-2}{\rm s}^{-1}{\rm sr}^{-1} \ . \tag{12}$$

3 SEARCH FOR PRIMARY IMPS

Our definition of a primary IMP is one that appears to be a *single* supermassive particle that travels through all 4 scintillation detectors, producing signals above threshold in each of the detectors. The primary IMP can either impinge upon the atmosphere and propagate through the remaining overburden to and through the IMAX gondola, or it can be produced by an impinging cosmic ray in the atmosphere or in the gondola shell above the first scintillation detector T1.

3.1 Negligible Velocity-Change Search

From the time-delays measured for each event, we compute the three velocities, along with the associated uncertainties. From each velocity, we compute the 'slowness' between detector i and detector $i+1$ as $s_i \equiv 1/v_i$, where v_i is the velocity measured between these detectors; slowness is measured in the units of μs/m. We use slowness as our primary variable rather than velocity because the background distributions for slowness are uniform (flat) as opposed to the background distributions for velocity which are proportional to v^{-2}.

From the three slownesses, we compute the weighted mean slowness, $\bar{s}$, and the weighted chi-squared

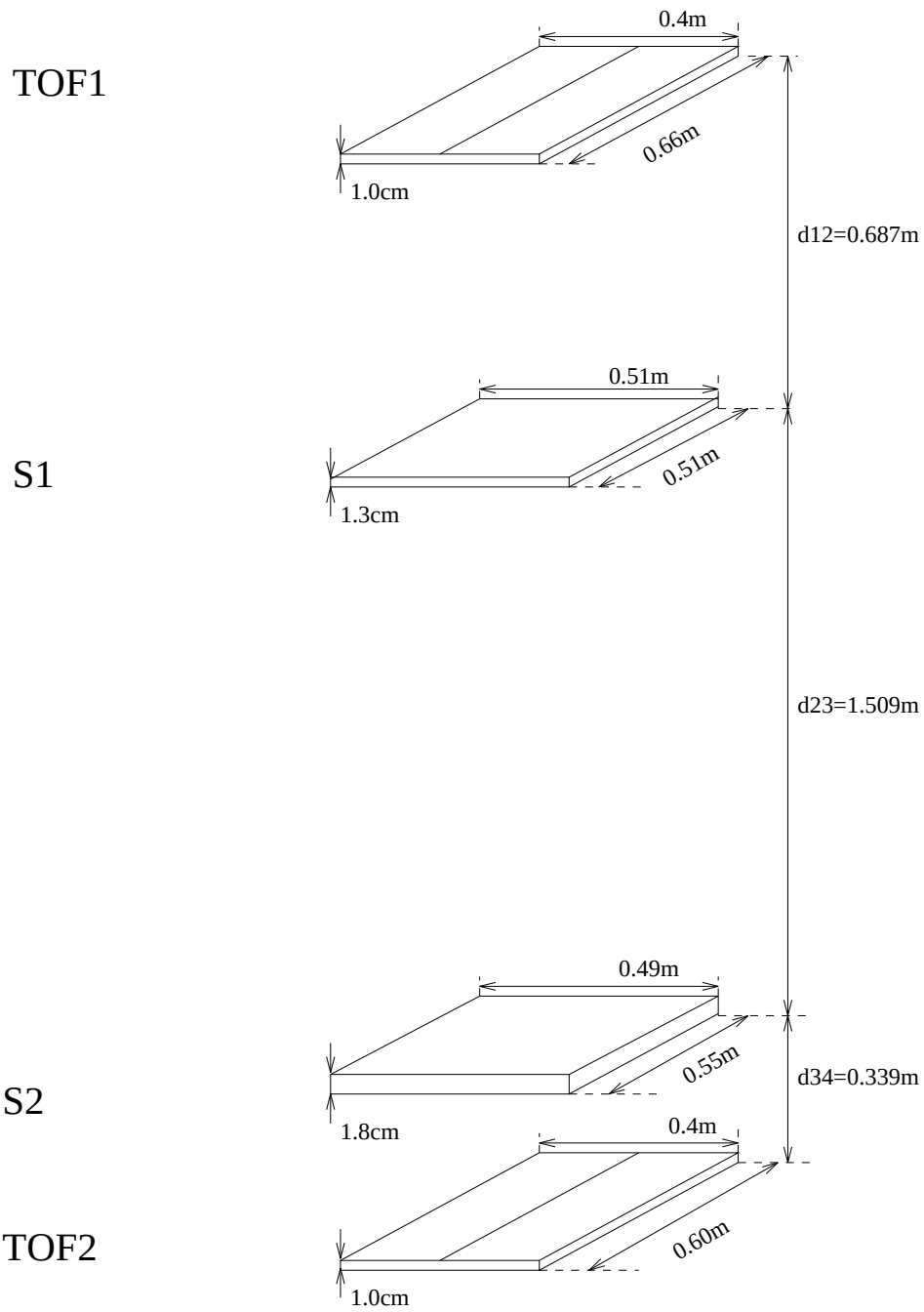

Figure 1: Diagram of IMAX Telescope, showing the positions and dimensions of the 4 scintillation detectors.

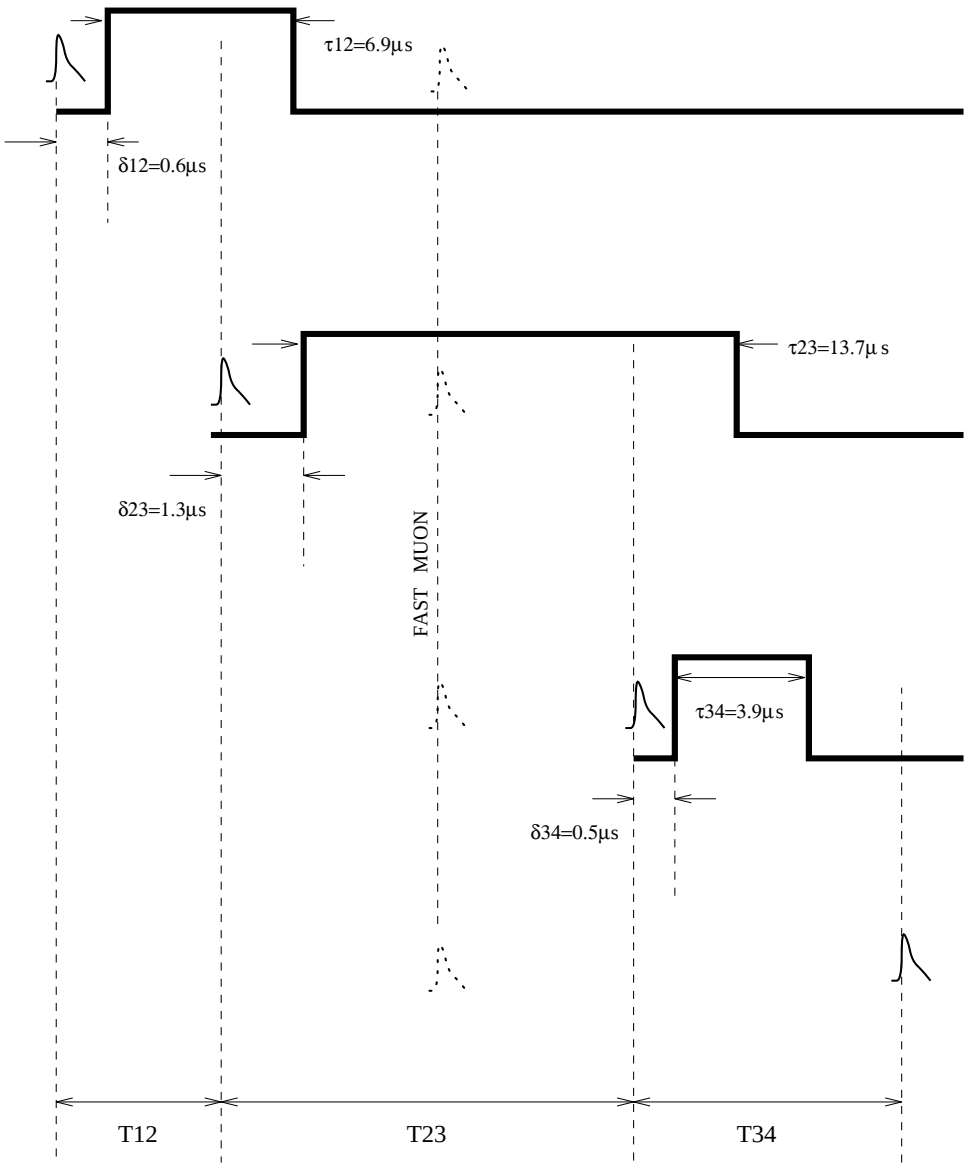

Figure 2: Delayed-coincidence timing diagram for 3 counters. For each successive gate, we indicate the gate-delay, $\delta_{i,i+1}$, and the gate-width, $\tau_{i,i+1}$. We also indicate the time delays, $T_{i,i+1}$, between intercounter pulses. The fourth counter is not included in the coincidence, but as long as there is a hit in the fourth counter during the τ_{34} gate, T_{34} is measured. If more than one counter has a hit within an anticoincidence gate of 200 ns, then all the participating counter pulses are vetoed, e.g., the indicated fast muon which went through all four detectors has been vetoed.

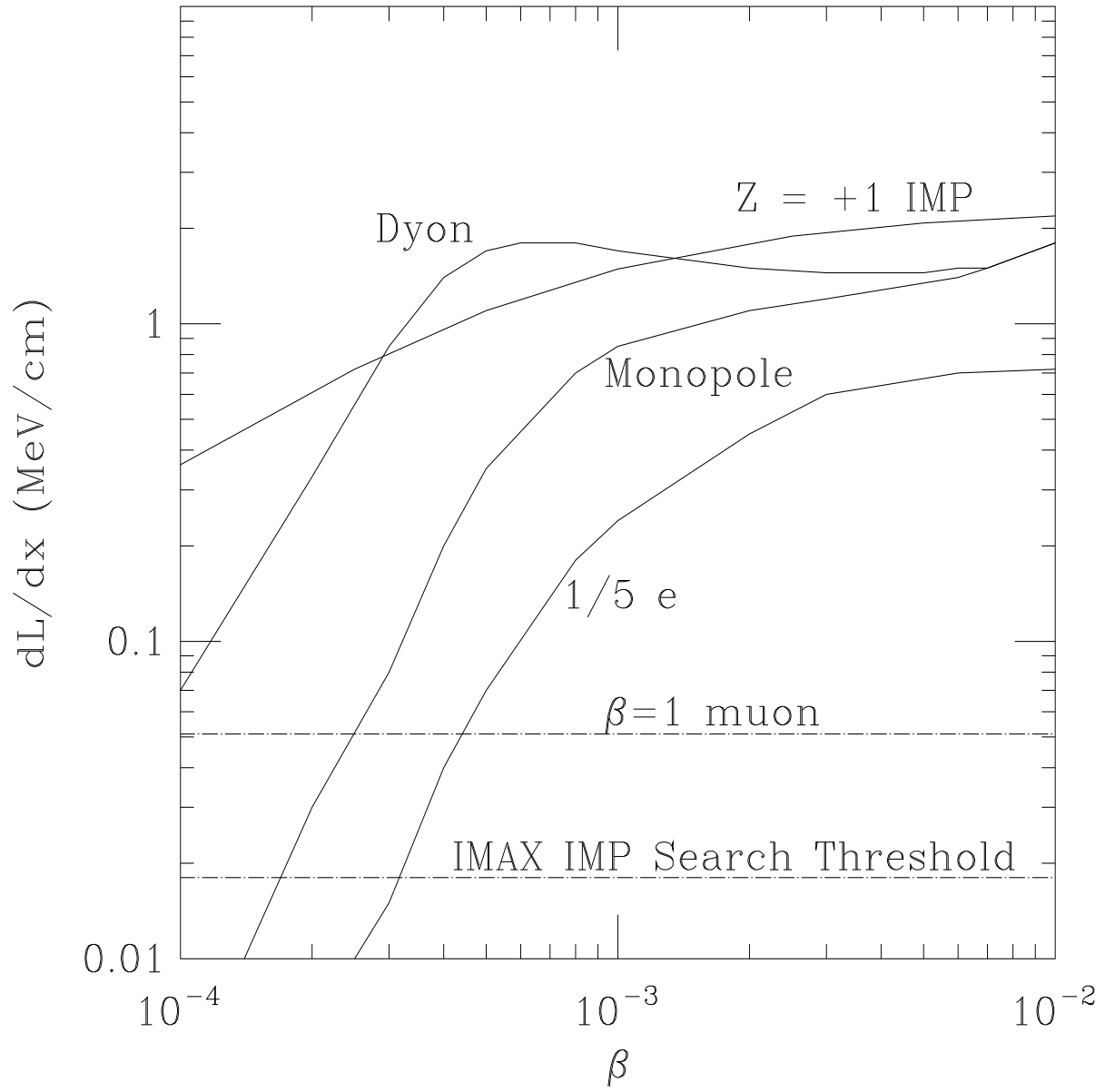

Figure 3: Specific light yield for $Z = +1$ IMPs, bare GUT monopoles, dyons (monopole-proton pair), and $\frac{1}{5}e$ supersting particles. Also indicated are the response for relativistic muons and the threshold for the IMAX experiment. Adapted from [47].

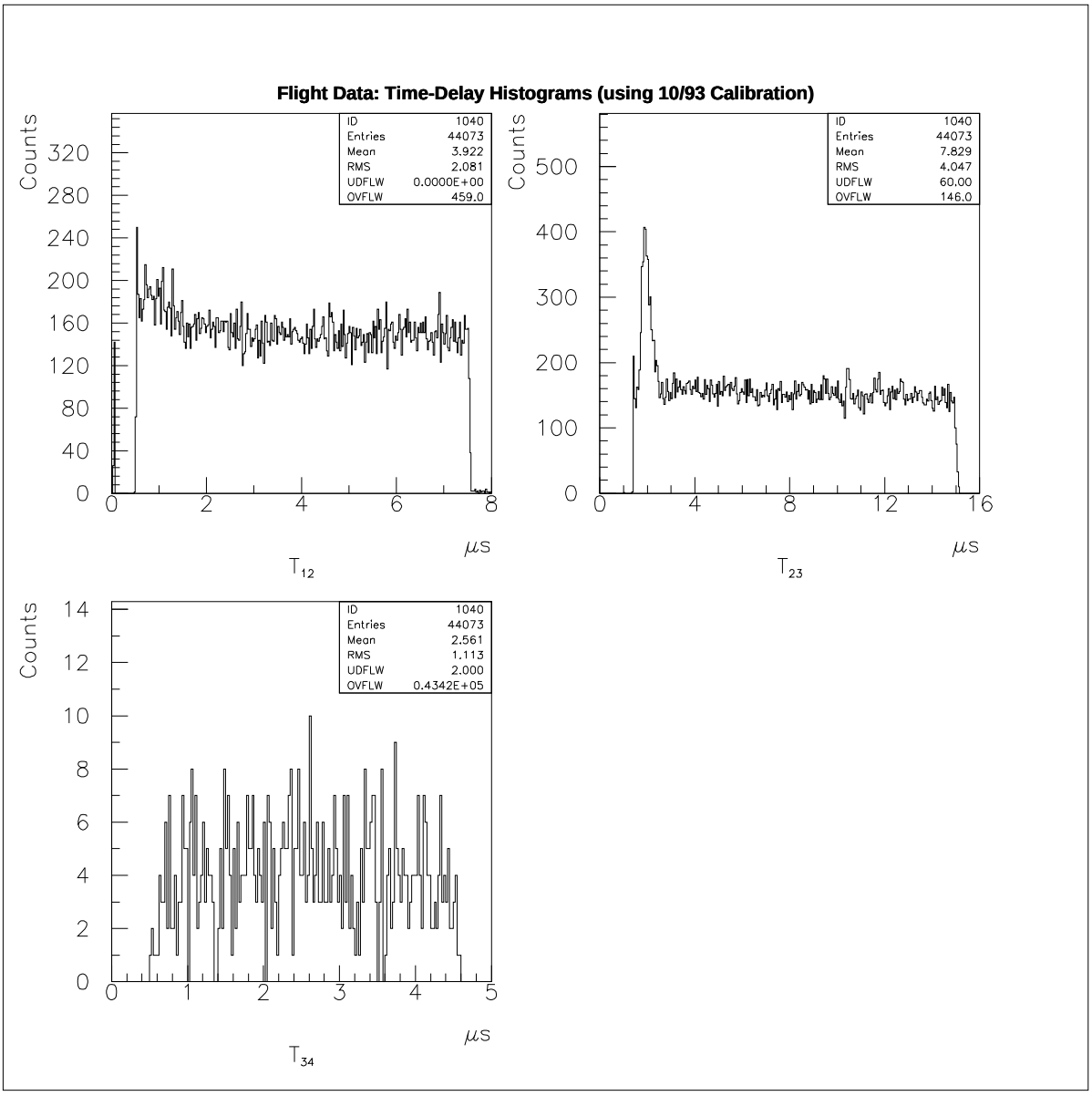

Figure 4: The IMAX flight time-delay histograms for the three time-delay channels show the expected flat distributions for accidental coincidences *plus* unusual structure for T_{12} and T_{23} near the beginning of the timing gates. This data consists of the float data (5 g/cm^2) which had CAMAC temperatures lower than 34.0° C, or equivalently UT $\in [10.0, 15.0]$ hours.

deviation from the mean , χ^2:

$$\begin{aligned} \bar{s} &= \frac{1}{W}\sum_{i=1}^{3}\frac{s_i}{\sigma_{s_i}^2} \\ \chi^2 &= \sum_{i=1}^{3}\frac{(s_i-\bar{s})^2}{\sigma_{s_i}^2} \quad , \end{aligned} \tag{13}$$

where W is given by:

$$W = \sum_{i=1}^{3}\frac{1}{\sigma_{s_i}^2} \quad . \tag{14}$$

If $\chi^2 < 2.5$, then the event is consistent with an IMP that passes through all four detectors without gaining any slowness, or equivalently, without slowing down.

We show the IMAX flight and Monte Carlo distributions of χ^2 (see Eq. 13) for the negligible-Δv search in Figure 5. From the IMAX flight distribution of χ^2 in Figure 5, we determine the number of background events, by averaging over all bins for $\chi^2 < 100$, to be 4.0 ± 0.3. If IMPs exist and deposit sufficient energy in each of the detectors without substantially slowing down, then we expect 70% of the IMP signal events to have $\chi^2 < 2.5$. The actual number of such signal events is 5, which corresponds to a 95% C.L. upper limit of 9.1 IMP events (by using Poisson statistics and a correction factor of 1.4 for IMP events with $\chi^2 \geq 2.5$). The results of the $\Delta v \approx 0$ search are summarized in Tables 2 and 3.

3.2 Large Velocity-Decrease Search

In a similar manner, we can search for IMPs that actually slow down slightly within the IMAX telescope. We hypothesize that the energy-loss for a given amount of material is a power-law in velocity:

$$\frac{dE}{dx} = -\alpha_n v^n \quad , \tag{15}$$

which implies that the slowness-gain (with $\gamma \equiv 3-n$) is:

$$\begin{aligned} \frac{ds}{dx} &= +\frac{\alpha_n}{M_x}s^{3-n} \\ &= +a_\gamma s^\gamma \end{aligned} \quad . \tag{16}$$

For $\gamma = 1$, the slowness as a function of the total material traversed is:

$$s_1(x) = s_0 \exp(a_1 x) \quad , \tag{17}$$

where s_0 is the slowness of the IMP at $x = 0$. For $\gamma \neq 1$, by solving equation 16, the functional form of slowness is:

$$s_{\gamma\neq 1}(x) = s_0\left(1-(\gamma-1)a_\gamma s_0^{\gamma-1}x\right)^{\frac{1}{1-\gamma}} \quad . \tag{18}$$

Hence, if we measure several slownesses as a function of x, for all γ, determination of s_0 and a_γ is a complicated solution to nonlinear equations (especially when there are unused detectors of significant grammage interspersed between the active detectors). However, for all γ, if $a_\gamma s_0^{\gamma-1}x << 1$, then:

$$s_\gamma(x) \approx s_0 + a_\gamma s_0^\gamma x \quad , \tag{19}$$

which is a much easier linear fitting problem, and permits a simple solution. The results of 'small-Δv' search, which requires no assumptions about the index γ, nor $n = 3-\gamma$, are listed in Tables 2 and 3; further details can be found in reference [41].

A large velocity-change IMP search is complicated by the significant amount of material between the scintillation detectors in IMAX. This causes the IMP velocity to decrease while the IMP is travelling through the inert material between the two detectors. Thus the measured velocity will be the weighted average of the instantaneous velocities between the different absorbers that lie between a pair of detectors. The measured slowness will be:

$$s_k = s_0\sum_{i=k'}^{k-1} f_{i,i+1}\exp\left(a_1\sum_{j=1}^{i}x_j\right), \tag{20}$$

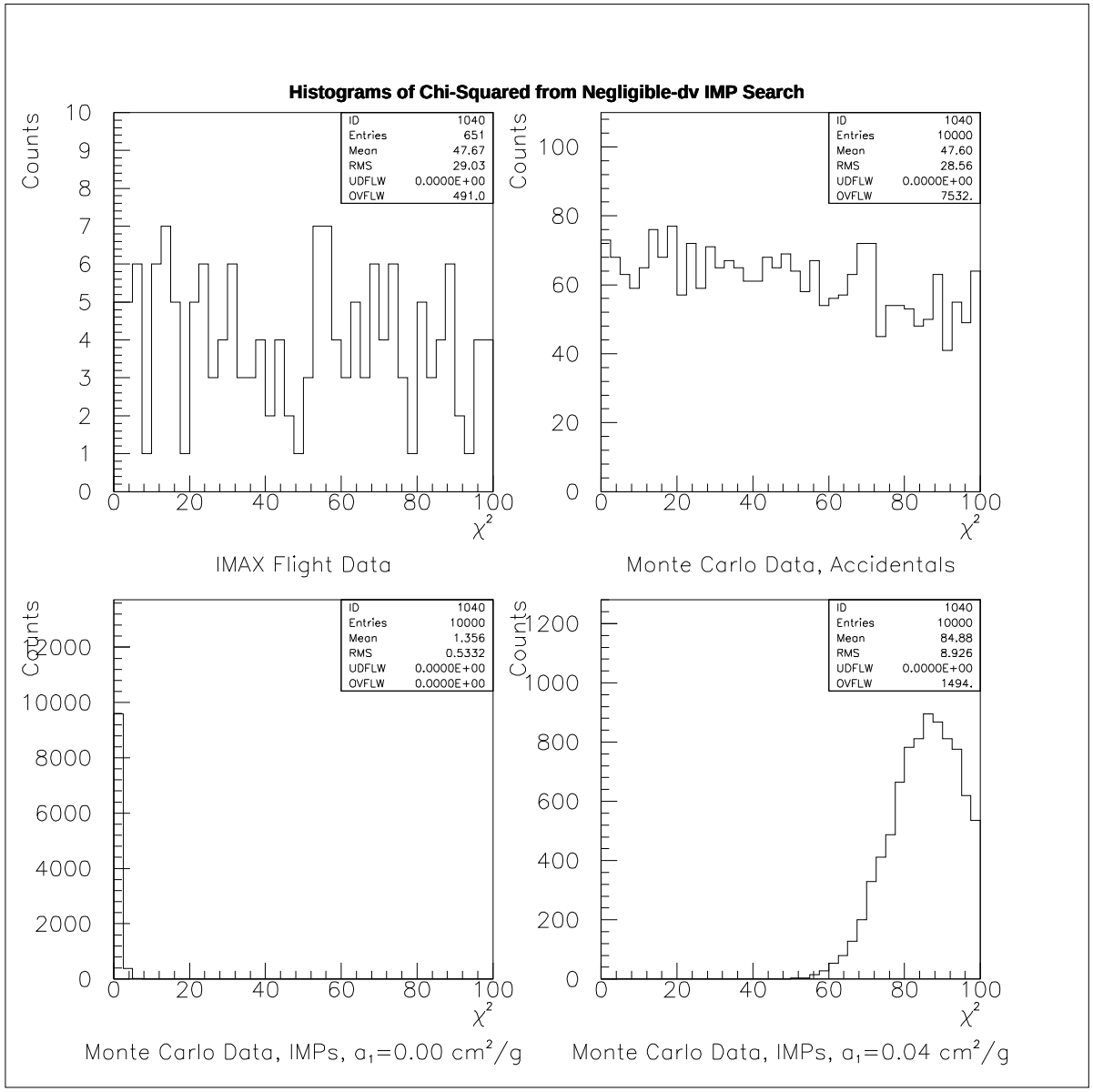

Figure 5: IMAX flight and Monte Carlo χ^2-distributions for fitting each four-fold coincident event to a constant velocity. For UT $\in [10.0, 15.0]$ hours, we checked each four-fold coincidence for consistency with a single particle that has travelled through all 4 scintillation detectors. We show the data from the IMAX flight, and from three separate Monte Carlos, one for purely accidental coincidences, and two for IMP-like events with different values of a_1 (see Section 3.3). If an event has $\chi^2 < 2.5$, then it is consistent with a constant velocity IMP. Note the flatness of the background for the $\Delta v = 0$ distribution up to $\chi^2 = 100$ in both the IMAX flight data and the simulated accidental coincidences.

where $f_{i,i+1} \equiv d_{i,i+1}/d_{1,i+1}$ is the fractional separation of neighboring 'absorbers', x_i is the thickness (in g/cm^2) of each absorber, and s_0 is the slowness of the IMP just prior to entering detector 1. The index k' represents the first detector in the pair of detectors used to measure the slowness; and the index k represents the second detector of this pair (i.e., for IMAX, the three (k',k) detector pairs are: (1,7), (7,11), and (11,12)). We define the s_k determined in Equation 20 as:

$$s_k \equiv s_0 \exp(a_1 \Delta), \tag{21}$$

where Δ is to be determined for each detector and absorber configuration. As long as

$$\mid a_1 \left(\sum_{j=1}^{i} x_j - \Delta \right) \mid \ll 1, \text{ for all } i \in [1,k], \tag{22}$$

then we can easily determine Δ:

$$\Delta(k) \approx \frac{1}{k} \sum_{i=1}^{k} \sum_{j=1}^{i} x_j. \tag{23}$$

With the values of $\Delta(n)$, we take the logarithm of both sides of Equation 21 and perform a *linear* regression on the 3 equations (one equation for each slowness measurement (s_7, s_{11} and s_{12})) to determine the best fit values of s_7^0 and a_1:

$$\ln(s_n) = a_1 \Delta(n) + \ln(s_7^0). \tag{24}$$

The case where $n = 2$ and $\gamma = 3 - n = 1$ is of special interest because neutral IMPs are usually assumed to have a transport cross-section $\sigma_{\rm trans}$ ($= \sigma$ for isotropic scattering) which is independent of β, which leads to

$$\frac{dE}{dx} = A \sigma_{\rm trans} \beta^2 c^2, \tag{25}$$

where $A = 1$ for cgs or SI units, or $A = 5.62 \times 10^{26}$ c^2/MeV for E in MeV, x in g/cm^2, $\sigma_{\rm trans}$ in cm^2, and $c = 1$. For this case ($\gamma = 1$, $n = 2$), the exponential form of equation 17 allows the statistical regression analysis to be linearized, even for large Δv. In a similar manner as used in the $\Delta v \approx 0$ and the small-Δv searches, we estimate an upper limit on the number of large-Δv IMPs by taking the number of counts in the first bin of the $\sqrt{\chi^2}$-histogram as the signal (16 events), and comparing this to the (assumed to be flat) background found by averaging the number of counts in the first 4 bins (18.25 ± 2.14 counts/bin). We only averaged over the first 4 bins due to the large bump in the physically allowed ($a_1 > 0$) $\sqrt{\chi^2}$-distribution for the accidental coincidence Monte Carlo at $\sim 8 \pm 3$. We then arrive at an upper limit on the number of IMP events during the 5 hour flight data set of 11.1 events (95% C.L.), where we have taken care to count the signal events that would reside in the second $\sqrt{\chi^2}$ bin (by multiplying the first bin result by 1.3).

3.3 Monte Carlo Simulations of the Searches

The accidental coincidence Monte Carlo is quite simple: we choose three time-delays each from a uniform distribution of a certain width. With these time-delays, we compute the time-delay uncertainties as we did for the actual data at 14.0 hours UT (the time-delay uncertainties are time-dependent). These time-delays and uncertainties served as the input variables to the same fitting procedures described above for the flight data.

The Monte Carlo for IMP-like events consisted first of choosing an input IMP speed, v, from a 'cut-off' Maxwellian distribution (equation 3)[4][32]. The second step of the IMP-like event Monte Carlo is to determine whether or not an IMP with this velocity and a pre-determined energy loss (a_γ) will produce time-delays that fall within the delayed coincidence gates. In order to determine whether an IMP will make these cuts, we propagate the IMP through the telescope using Equations 17 and 20 (for $\gamma = 1$).

With the IMP Monte Carlo, we can input different values of a_1 to determine the smallest a_1 where each of the IMP searches ($\Delta v \approx 0$, small-Δv, and large-Δv) fail. We found that for $a_1 < 0.013$ cm^2/g, all the searches perform as advertised, giving values of $\chi^2 < 2$ and positive values for the fitted a_1 and s_0. For $a_1 = 0.013$ cm^2/g, the negligible velocity change search fails for the first time, giving $\chi^2 > 8 \pm 5$, with very few events in the first bin of the χ^2-histogram, $\chi^2 < 2.5$. When $a_1 = 0.07$ cm^2/g, the small-Δv search fails, giving unphysical, negative values for the fitted parameters a_1 and s_0, though the χ^2

values were still acceptably small ($\sqrt{\chi^2} < 2.5$). At $a_1 = 0.24$ cm^2/g, the large-Δv IMP search fails, giving $\sqrt{\chi^2} = 6 \pm 1$. However, this failure of the large-Δv search does not affect our results because the velocities of the dark matter Maxwellian distribution are too small. For $a_1 \geq 0.123$ cm^2/g, all of the IMPs (with velocities less than the galactic escape velocity of $v_{\max} = 640$ km/s) get stopped in the atmosphere or gondola shell (The overburden at float altitude is 5 g/cm^2 for the atmosphere and 1.08 g/cm^2 for the aluminum gondola shell) above the IMAX detectors. The velocities of the IMPs above the atmosphere were chosen from a cutoff Maxwellian distribution (Equation 3). The velocity of the IMPs ($n = 2$) degrades exponentially with the thickness of the atmospheric overburden. Since the IMPs have initial velocities $v < 640$ km/s, a large value of a_1 will soon degrade the velocities to be below our minimum velocity of $v \sim 100$ km/s. For no velocity degradation ($a_1 = 0.00$ cm^2/g), only 2.2% of the events are lost from this Maxwellian distribution due to the D-module timing cuts. However, when $a_1 = 0.08$ cm^2/g, the D-module does not detect 59.7% of the Maxwellian distribution since the lower velocity IMPs slow down significantly in the atmosphere and the measured time-delays will be too long for the D-module's time-delay cuts. When $a_1 \geq 0.123$ cm^2/g, none of the IMPs from the cutoff Maxwellian velocity distribution have a large enough velocity to satisfy the D-module detector cuts after propagating through the atmosphere and gondola. This maximum value of a_1 corresponds to a maximum cross-section to mass ratio of $\sigma_1/m_x = 2.2 \times 10^{-25}$ cm^2/GeV, and will be used to place constraints on IMPs. As a point of warning, due to our uncertainty of the response of plastic scintillators to low velocity particles, we did not include the D-module's discriminator thresholds when we computed the fraction of events accepted. However, if a theoretical model can be developed for the efficiency for light production by *carbon* recoils, then with the results discussed in Section 2, we can easily include the light yield and the discriminator thresholds in the IMP Monte Carlo.

4 IMPLICATIONS OF IMAX IMP SEARCH

The results of the IMAX IMP search are summarized in Tables 2 and 3 and Figure 6. The boundaries of the IMAX-constrained region have simple explanations:

- The discriminator for detector S2 had the highest setting of the four discriminators, at an energy loss of $dE/dx \sim 3.5$ MeV/g/cm^2, which corresponds to a transport cross-section of:

$$\sigma = \frac{1}{v^2}\frac{dE}{dx} \sim 6.23 \times 10^{-21} \text{ cm}^2, \tag{26}$$

  where $v \sim 300$ km/s.

- IMPs with $\sigma/m_x < 2.1 \times 10^{-25}$ cm^2/GeV will lose less than $1 - \exp(-0.123 \times 18.82) \sim 90.1\%$ of their velocity while traveling through the atmosphere and the IMAX telescope. Our analysis indicates that during the five hours of quality data acquisition at high altitude, we observed < 11.1 large-Δv slowing events consistent with these cross-sections (or an upper limit on the flux of 7.9×10^{-6} cm^{-2}s^{-1}sr^{-1}, which corresponds to $m_x \geq 1.3 \times 10^{11}$ GeV for $f_d = 1$).

The IMAX constrained regions of IMP parameter space are indeed quite useful. We are the *first* experiment to search for IMPs in the triangle of parameter space with cross-sections $\sigma \in [7 \times 10^{-21}, 10^{-18}]$ cm^2, masses $m_x > 10^7$ GeV, and slowing-rates $\sigma/m_x > 10^{-28}$ cm^2/GeV. For $m_x < 10^7$ GeV, $\sigma > 7 \times 10^{-21}$ cm^2, and $\sigma/m_x < 2.1 \times 10^{-21}$ cm^2/GeV, our experiment can constrain f_d to be five orders of magnitude lower than published experimental limits[7][25]. We achieve this high sensitivity by using a delayed coincidence between multiple detectors to reject the cosmic ray background, which prior dark matter searches at high altitude have been unable to accomplish.

When we actually assume a specific IMP-nucleus interaction model to parametrize the different IMP scattering cross-sections with different nuclei, we indeed find that our IMP search does place useful *new* constraints on IMP parameter space, closing the wide-open windows in parameter space ($m_x > 10^6$ GeV). The windows shown here are from the Starkman *et al.* interpretation[25], adapted from and including the results of the recent BPRS publication[19]. The BPRS collaboration was able to chip away about half of the previously larger window W_2 for the spin-dependent interactions, but they were unable to further constrain the window W_2 for coherent interactions. We effectively eliminate the small remaining window W_2 for the spin-dependent IMP-nucleus interactions, and a large fraction of the remaining window W_2

for the coherent IMP-nucleus interactions. The remaining portion of the window W_2 can be constrained by a sea level IMP search with low thresholds and a significant background rejection capability.

For our experiment, we estimate the $\mathcal{F}$ factors (see Ref. [25]) for IMP propagation down to and including detector S2 by using the atomic composition of the detectors, gondola, and air. We find that for the IMAX experiment that $\bar{\mathcal{F}} \approx 170$ for spin-dependent interactions, and $\bar{\mathcal{F}} \approx 1.4 \times 10^5$ for coherent interactions (where the bar represents a weighted average over all the detectors and absorbers, the gondola-shell and the air above the payload). The $\bar{\mathcal{F}}$ factors serve to redefine the raw cross-section into a proton cross-section equivalent for the maximum detectable cross-section to mass ratio (the upper diagonal lines of the IMAX-constrained regions in Figure 6). We also compute $\mathcal{F}$ detectors for the plastic scintillation detectors: $\mathcal{F} \approx 1.5$ for spin-dependent interactions and $\mathcal{F} \approx 1.7 \times 10^4$ for coherent interactions. We apply these plastic scintillator $\mathcal{F}$ values to the least sensitive IMAX detector (S2) (with a threshold of $dE/dx = 3.5$ MeV cm^2/g) to determine the minimum detectable IMP cross-section for coherent and spin-dependent interactions (the lower horizontal lines of the IMAX-constrained regions in Figure 6).

We find that our results constrain monopoles, neutral hadronic matter and neutraCHAMPs with the first direct search in the mass range $m_x \in [\sim 10^6, \sim 10^8]$ GeV. Of course, these particles have been searched for indirectly before, via astrophysical reasoning (e.g., the exquisite Parker limit for monopoles; cannibalization of neutron stars by CHAMP black holes[27]) or via experiment[4][6][9]. But a direct search, like our balloon-borne multiple plastic scintillation detector search, often has the advantage of model independence over the usual strong model dependence of an indirect search. For example, our direct IMP search can in principle detect several wildly different types of particles (monopoles, CHAMPs, strange quark nuggets, neutraCHAMPs), while the most indirect searches can only detect a single particle species.

The results tabulated in Tables 2 and 3 should be in such form to facilitate re-interpretation of our results (such as more sophisticated explorations of f_d, σ, and m_x parameter space), should new data on the dark matter problem become available in the future. If one wants to place constraints on a specific particle model for IMPs (e.g., monopoles, neutraCHAMPs, strange quark nuggets), then one should take caution: the large-Δv search results only apply to those particles with dE/dx proportional to v^2 (e.g., strange quark nuggets, supermassive neutrons), while the small-Δv search applies to particles with energy loss proportional to any power of v (i.e. $dE/dx = Cv$, as in the case of neutraCHAMPs slowing in a classical r^4 nuclear dipole potential, or for the Ahlen-Kinoshita monopole energy loss formalism).

References

[1] K.C. Freeman, In **Dark Matter in the Universe**, eds. J. Kormendy and G.R. Knapp (D. Reidel, Dordrecht), p. 119 (1987).

[2] M. Schmidt, In *The Milky Way Galaxy* (IAU Symposium 106), eds. H. van Woerden *et al.*, (Reidel, Dordrecht), p. 75 (1985).

[3] R.A. Flores, *Phys. Lett.* **B215** 73 (1987).

[4] S.W. Barwick, P.B. Price, and D.P. Snowden-Ifft, *Phys. Rev.* **L64**, 2859 (1990).

[5] D.O. Caldwell, *Nucl.Phys.* **B28A** *(Proc. Suppl.)*, 273 (1992).

[6] Snowden-Ifft and Price, *Phys. Lett.* **B288**, 250 (1992).

[7] J. Rich, R. Rocchia, and M. Spiro, *Phys. Lett.* **B194**, 173 (1987).

[8] Snowden-Ifft, Barwick, and Price, *Astrophys. J.* **L364**, 25 (1990).

[9] J.H. Adams, R.L. Kinzer, W.N. Johnson, and J.D. Kurfess,*Naval Research Laboratory Preprint* (1989).

[10] J.L. Basdevant, R. Mochkovitch, J. Rich, M. Spiro, and A. Vidal-Madjar,*Phys. Lett.* **B234**, 395 (1990).

[11] J.I. Collar and F.T. Avignone III, *Phys. Lett.* **B275**, 181 (1992).

Number of scintillation counters	4
Total thickness of counters	5 g/cm^2
Total thickness of material above counter telescope (including 5 g/cm^2 atmosphere)	6 g/cm^2
Total thickness of material between counters	8 g/cm^2
Total thickness to reach and traverse experiment	19 g/cm^2

Geometry factor	$\Omega = 100$ cm^{2}sr
Time at float altitude (for high quality DM data)	$t = 1.8 \times 10^4$ seconds
IMP velocity range	$\beta = (0.33 \text{ to } 3.3) \times 10^{-3}$ $[v = (0.1 \text{ to } 1)\text{m}/\mu\text{s}]$

Trigger thresholds in 1 cm plastic scintillators:
$\beta \approx 1, Z = \pm 1$, 35% of Landau peak of minum-ionizing particles in 1 cm; $dL/dx = 0.018$MeV/cm
$Z = +1$ IMPs (includes X^+ and $X^- - -\alpha$ CHAMPs), monopoles, dyons, $(1/5)e$ superstring particles are all above thrshold over full IMP velocity range listed above (see Figure 3)

Table 1: Parameters of IMAX Balloon-Borne Experiment

Search	$\frac{dE}{dx}(THR)$	$\sigma_{\min}(\mathbf{cm}^2)$	$a_1^{\max}$ $(\frac{\text{cm}^2}{g})$	$(\frac{\sigma}{m_x})^{\max}$ $(\frac{\text{cm}^2}{\text{GeV}})$	$\mathbf{A\Omega}$ $\mathbf{(cm^2 sr)}$
$\Delta v \approx 0$	3.0	6.2×10^{-21}	0.013	2.31×10^{-26}	100
small Δv	3.0	6.2×10^{-21}	0.07	1.2×10^{-25}	100
large Δv	3.0	6.2×10^{-21}	0.123	2.1×10^{-25}	100
Triples	3.0	6.2×10^{-21}	0.123	2.1×10^{-25}	135
Singles Rate	0.9	1.6×10^{-21}	0.38	3.3×10^{-25}	9120

Table 2: Summary of IMAX Results, part 1. For each IMP search, we tabulate the energy loss detection threshold ($dE/dx(THR)$($\mathbf{MeV/g/cm^2}$)), the corresponding threshold cross-section including the β^2-dependence of dE/dx ($\sigma_{\min}$), the maximum slowing down rate ($a_1^{\max}$), the corresponding maximum elastic cross-section to mass ratio ($(\sigma/m_x)^{\max}$), and the geometry factor ($\mathbf{A\Omega}$) for the search. The incident velocity acceptance for the searches was nominally $v_0 \in [99.6, 752]$ km/s (for high slowing down rates, larger initial velocities were acceptable).

Search	**N**	**B**	$n_{s,\max}$	$\phi_{\max}(\frac{1}{\text{cm}^2\,\text{s}\,\text{sr}})$	$m_{\max}$ **(GeV)**
$\Delta v \approx 0$	5	4.0 ± 0.3	9.1	6.5×10^{-6}	1.5×10^{11}
small-Δv	5	7.5 ± 0.1	6.9	4.9×10^{-6}	2.0×10^{11}
large-Δv	16	18.3 ± 2.1	11.1	7.9×10^{-6}	1.3×10^{11}
Triples	4 Hz	0 Hz	4 Hz	3×10^{-2}	3.3×10^{7}
Singles	4000 Hz	0 Hz	4000 Hz	0.44	2.27×10^{6}

Table 3: Summary of IMAX Results, part 2. For each IMP search, we tabulate the number of signal (**N**) and background (**B**) events observed, the 95% C.L. Poisson upper limit ($n_{s\max}$) on the number of IMP events, the upper limit on the flux ($\phi_{\max}$), and the maximum mass detectable ($m_{\max}$) (assuming IMPs are all the dark matter).

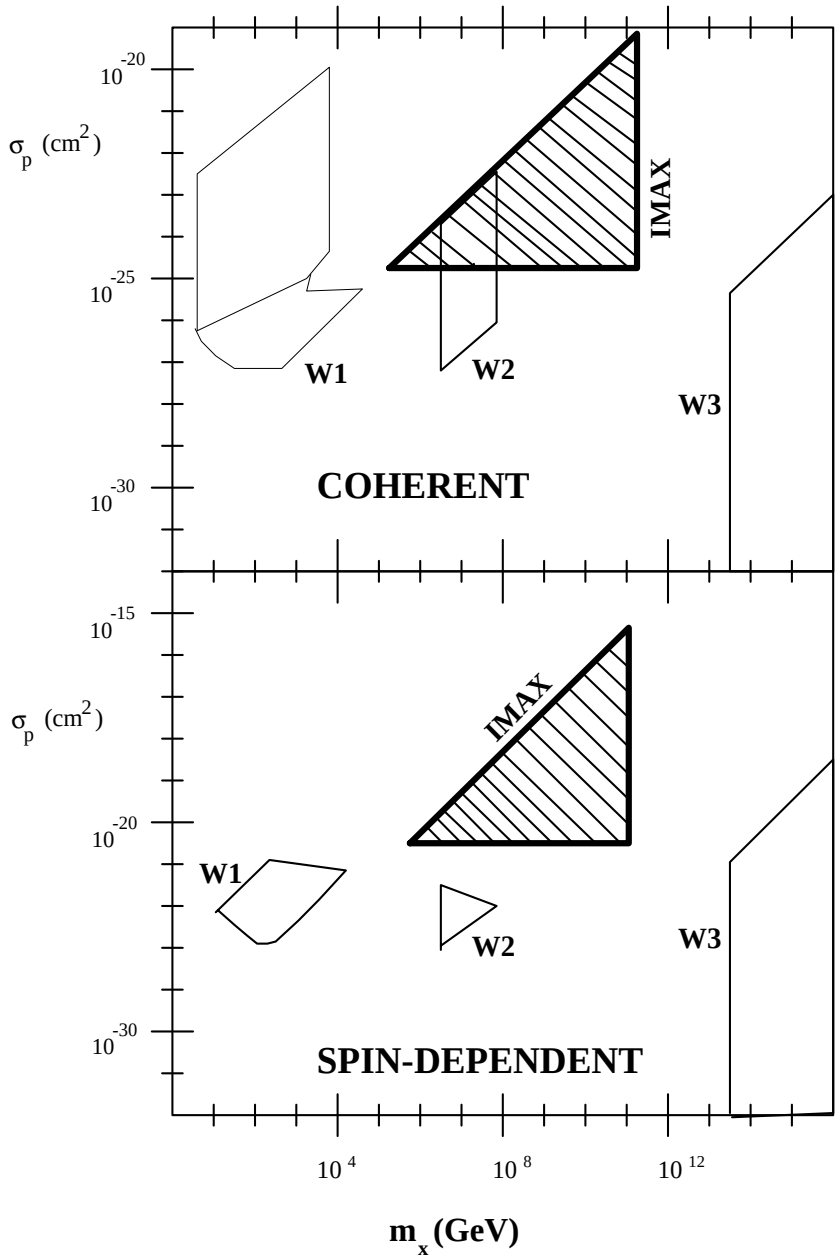

Figure 6: We show the IMAX constraints on the SIMP mass/cross-section parameter space for coherent interactions and for spin-dependent interactions. Without the IMAX results, there are three different non-excluded windows in each parameter space W_1, W_2, and W_3. The hatched areas are the IMAX excluded regions, assuming that SIMPs are all the galactic halo dark matter ($f_d = 1$).

[12] B. Barish, G. Liu, and C. Lane, *Phys. Rev.* **D36**, 2641 (1987).

[13] T. Tsukamoto *et al.*,*Europhys. Lett.* **3**, 39 (1987).

[14] E.K. Shirk and P.B. Price, *Astrophys. J.* **220**, 719 (1978).

[15] Robert N. Cahn and Sheldon L. Glashow, *Science* **213**,607 (1981).

[16] Eric B. Norman, Stuart B. Gazes, and Dianne A. Bennett, *Phys. Rev. Lett.* **58**, 1403 (1987).

[17] G. Liu and B. Barish, *Phys. Rev. Lett.* **61**, 271 (1988); T. Saito, Y. Hatano, Y. Fukada, H. Oda, *Phys. Rev. Lett.* **65**, 2094 (1990); S. Ahlen *et al.*, *Phys. Rev. Lett.* **69**, 1860 (1992).

[18] S. Orito, H. Ichinose, *et al.*, *Phys. Rev.* **L66**, 1951 (1991).

[19] C. Bacci, P. Belli, R. Bernabei, *et al.* (BPRS Collaboration), *LNGS-93/80, DAPNIA/SPP-93-16 Preprint* (1993), to appear in Astroparticle Physics (1994).

[20] A. De Rujula, S.L. Glashow, and U. Sarid, *Nucl. Phys.* **B333**, 173 (1990).

[21] A. DeRujula and S.L. Glashow, *Nature* **312**, 734 (1984).

[22] Stephen Wolfram, *Phys. Lett.* **B82**, 65 (1979).

[23] Mark W. Goodman and Edward Witten, *Phys. Rev.* **D31**, 3059 (1985).

[24] H. Goldberg and L.J. Hall, *Phys. Lett.* **B174**, 151 (1988).

[25] G.D. Starkman, A. Gould, R. Esmailzadeh, S. Dimopoulos,*Phys. Rev.* **D41**, 3594 (1990).

[26] S. Dimopoulos, D. Eichler, R.Esmailzadeh, and G.D. Starkman, *Phys. Rev.* **D41**, 2388 (1990).

[27] A. Gould, B.T. Draine, R.W. Romani, and S. Nussinov,*Phys. Lett.* **B238**, 337 (1990).

[28] R.S. Chivukula, A.G. Cohen, S. Dimopoulos, and T.P. Walker, *Phys. Rev.* **L65**, 957 (1990).

[29] I. Goldman and S. Nussinov, *Phys. Rev.* **D40**, 3221 (1989).

[30] Kim Griest and Marc Kamionkowski, *Phys. Rev. Lett.***64**, 615 (1990).

[31] E. Witten, *Phys. Rev.* **D30**, 272 (1984).

[32] J.R. Primack, D. Seckel and B. Sadoulet, *Ann. Rev. Nucl. Part. Sci.* **38**, 751 (1988).

[33] B. Paczynski, *Astrophys. J.* **304**, 1 (1986).

[34] C. Alcock *et al.* (MACHO Collaboration), *Nature* **365**, 621 (1993).

[35] E. Aubourg *et al.* (EROS Collaboration), *Nature* **365**, 623 (1993).

[36] J.A. Holtzman and J.R. Primack, *Astrophys. J.* **429** (1993).

[37] P.J. Kernan and L.M. Krauss, *Preprint CWRU-P2-94* (1994).

[38] Patrick McGuire and Theodore Bowen, *Proc.*
23rd International Cosmic Ray Conference (ICRC), Vol.4, p.726, Calgary (1993).

[39] J.W. Mitchell *et al.*, *Proc. 23rd ICRC*, Vol.1, p.519, Calgary (1993).

[40] McGuire, Bowen, L.M. Barbier, *et al.*, (The IMAX Collaboration),
Proc. 23rd ICRC, Vol.4, p.621, Calgary (1993).

[41] P.C. McGuire, *Ph. D. Dissertation*, University of Arizona, unpublished (1994).

[42] J. Lindhard, M. Scharff, H.E. Schiøtt,*Mat. Fys. Dan. Vid. Selsk.* **33**, No. 14 (1963).

[43] S. Ahlen, F.T. Avignone, *et al. Phys. Lett.* **B195** 603 (1987).

[44] D.J. Ficenec, S.P. Ahlen, *et al.*, *Phys. Rev.* **D36**, 311 (1987).

[45] J.A. Harvey and N.W. Hill, *Nucl. Instr. Meth.* **162**, 507 (1979).

[46] Ahlen and Tarlé, *Phys. Rev.* **D27**, 688 (1983).

[47] S.P. Ahlen, T.M. Liss, C. Lane and G. Liu, *Phys. Rev. Lett.* **55**, 181 (1985).

[48] D.L. Smith, R.G. Polk and T.G. Miller,*Nucl. Instr. Meth.* **64**, 157 (1968).

[49] H.J.Komori, *J.Phys.Soc.Japan*, **17**, 620 (1962).